

## Chapter 3

# On nonlinear singularly perturbed parameterized problems with integral boundary condition<sup>2</sup>

In this chapter, we consider the following class of nonlinear singularly perturbed parameterized problem with integral boundary condition: Find  $(u, \lambda)$  such that

$$\begin{cases} \mathcal{T}_\lambda u := \varepsilon u'(t) + f(t, u(t), \lambda) = 0, & t \in J = (0, 1], \\ u(0) + \int_0^1 c(s)u(s) ds = A, \\ u(1) = B, \end{cases} \quad (3.1)$$

where  $A$  and  $B$  are given constants,  $0 < \varepsilon \ll 1$  is the ‘singular perturbation parameter’ and  $\lambda$  is known as the ‘control parameter’. We assume that the functions  $c(t) > 0$  and  $f(t, u(t), \lambda)$  are sufficiently smooth in  $\bar{J} = J \cup \{0\}$  and  $\bar{J} \times \mathbb{R}^2$ , respectively. Moreover,

$$\beta \leq \frac{\partial f}{\partial u} \leq \beta^*, \quad \text{and} \quad \delta \leq \left| \frac{\partial f}{\partial \lambda} \right| \leq \delta_*, \quad (3.2)$$

for some positive constants  $\beta, \beta^*, \delta$  and  $\delta_*$ . Under these conditions, problem (3.1) has a unique solution  $\{u, \lambda\}$  on  $\bar{J}$ , and  $u$  possesses a boundary layer at  $t = 0$ .

Since a separate analysis is discussed for both Shishkin and Bakhvalov meshes in [79, 80], it is natural to ask if a general framework can be derived based on which parameter-uniform convergence of the scheme can be discussed on various a priori

---

<sup>2</sup>This chapter contains material published in *Numerical Algorithms*, 89, 791–809, 2022, doi: <https://doi.org/10.1007/s11075-021-01134-5>.

chosen layer adapted meshes, including both Shishkin and Bakhvalov meshes. We address this as a secondary goal of this chapter. Such a framework is previously developed in [2, 10, 68, 100] for various classes of singularly perturbed problems with Dirichlet boundary conditions.

The primary goal of this chapter is to establish an a posteriori error estimate in the maximum norm for problem (3.1). The a posteriori error estimate derived in this chapter can be used to design an adaptive procedure; we follow [43] for this purpose. We note that substantial work has been reported in research literature on a posteriori error estimation for singularly perturbed problems with Dirichlet boundary conditions, however with integral boundary conditions, we are aware of only [70] where the authors considered the following quasilinear singularly perturbed problem

$$\begin{cases} \mathcal{L}u := \varepsilon u' + f(t, u(t)) = 0, & t \in J = (0, 1], \\ u(0) = \mu u(1) + \int_0^1 b(s)u(s)ds + d, \end{cases} \quad (3.3)$$

where  $0 < \varepsilon \leq 1$  is the perturbation parameter, and  $\mu$  and  $d$  are given constants. The functions  $b$  and  $f$  are assumed to be sufficiently smooth in  $\bar{J}$  and  $\bar{J} \times \mathbb{R}$ , respectively. Further, it is assumed that

$$\beta^* \geq \frac{\partial f}{\partial u} \geq \beta > 0, \quad \text{in } \bar{J} \times \mathbb{R}.$$

Note that (3.1) and (3.3) are different classes of problems. The authors in [70] derived a posteriori error estimate for a finite difference discretization of (3.3). Unfortunately, there is a flaw in the analysis of [70]. We found that the authors did not take care of the integral boundary condition properly while discussing the a posteriori error estimate. For more details, see Remark 3.1 and the proof of Theorem 3.3. In this chapter, we have dedicated a whole section to rectify the shortcomings of a

posteriori error estimation in [70].

The outlines of the present chapter are as follows. In Section 3.1, we discuss the stability of the continuous problem (3.1). In Section 3.2, we describe a finite difference discretization of problem (3.1) on arbitrary meshes. In Section 3.3, we give a priori error estimate for the discrete problem; while, in Section 3.4, a posteriori error estimate is given. Section 3.5 is devoted to a posteriori error estimation for problem (3.3). Numerical results are presented in support of the theory in Section 3.6. Finally, the chapter ends with some concluding remarks in Section 3.7.

### 3.1 Stability of the continuous problem

The following lemma ensures that the solution  $\{u, \lambda\}$  of problem (3.1) is parameter-uniform stable.

**Lemma 3.1.** *For the solution  $\{u, \lambda\}$  of problem (3.1) it holds*

$$\max \{\|u\|_\infty, |\lambda|\} \leq C (|A| + |B| + \|F\|_\infty), \quad (3.4)$$

where  $F(t) = -f(t, 0, 0)$ .

**Proof.** The quasilinear problem (3.1) can be rewritten in linearized form as follows

$$\begin{cases} \varepsilon u'(t) + a(t)u(t) - \lambda b(t) = F(t), & t \in J = (0, 1], \\ u(0) + \int_0^1 c(s)u(s) ds = A, \\ u(1) = B, \end{cases} \quad (3.5)$$

where  $a(t) = f_u(t, \gamma u, \gamma \lambda)$ ,  $b(t) = -f_\lambda(t, \gamma u, \gamma \lambda)$  with  $0 < \gamma < 1$ . Using (3.5), it is established (3.4) in [79, Lemma 2.1]. □

The following lemma will be used in the derivation of a posteriori error estimate in Section 3.4.

**Lemma 3.2.** *For any  $(y_1, \eta)$  and  $(y_2, \nu)$  such that  $y_1(1) = y_2(1)$ ,*

$$(y_1 - y_2)(0) + \int_0^1 c(s)(y_1 - y_2)(s)ds = \zeta,$$

and

$$\mathcal{J}_\eta y_1 - \mathcal{J}_\nu y_2 = \varphi,$$

where  $\varphi$  and  $\zeta$  are bounded piecewise continuous functions, we have

$$\max\{\|y_1 - y_2\|_\infty, |\eta - \nu|\} \leq C(\|\varphi\|_\infty + |\zeta|).$$

**Proof.** Let us consider any  $(y_1, \eta)$  and  $(y_2, \nu)$  such that

$$(y_1 - y_2)(1) = 0, \tag{3.6}$$

$$(y_1 - y_2)(0) + \int_0^1 c(s)(y_1 - y_2)(s) ds = \zeta, \tag{3.7}$$

and

$$\begin{aligned} \varphi = \mathcal{J}_\eta y_1 - \mathcal{J}_\nu y_2 &= \varepsilon(y_1 - y_2)'(t) + f(t, y_1(t), \eta) - f(t, y_2(t), \nu) \\ &= \varepsilon(y_1 - y_2)'(t) + \widehat{a}(t)(y_1 - y_2)(t) - (\eta - \nu)\widehat{b}(t), \end{aligned} \tag{3.8}$$

where  $\widehat{a}(t) = f_u(t, y_2 + \gamma(y_1 - y_2), \nu + \gamma(\eta - \nu))$  and  $\widehat{b}(t) = -f_\lambda(t, y_2 + \gamma(y_1 - y_2), \nu + \gamma(\eta - \nu))$  for some  $0 < \gamma < 1$ . Thus, we can use Lemma 3.1 to obtain

$$\begin{aligned} \max\{\|y_1 - y_2\|_\infty, |\eta - \nu|\} &\leq C(|\zeta| + |0| + \|\varphi\|_\infty) \\ &= C(|\zeta| + \|\varphi\|_\infty). \end{aligned} \tag{3.9}$$

Hence, the proof is done. □

## 3.2 Discretization

Let us consider an arbitrary non-uniform mesh  $\bar{\omega} \equiv \{0 = t_0 < \dots < t_N = 1\}$  on  $\bar{J}$ . We define the mesh widths as  $h_j = t_j - t_{j-1}$  for  $1 \leq j \leq N$ . Consider  $U$  as the approximation of the exact solution  $u$ . On  $\bar{\omega}$ , for any mesh function  $v$ , we define

$$D^-v_j = \frac{v_j - v_{j-1}}{h_j}.$$

Integration of problem (3.1) over  $(t_{j-1}, t_j)$  gives

$$\varepsilon D^-u_j + h_j^{-1} \int_{t_{j-1}}^{t_j} f(t, u(t), \lambda) dt = 0.$$

Now apply the right rectangle rule to get

$$\varepsilon D^-u_j + f(t_j, u_j, \lambda) + R_j = 0 \tag{3.10}$$

with

$$R_j = -h_j^{-1} \int_{t_{j-1}}^{t_j} (t - t_{j-1}) \frac{d}{dt} f(t, u(t), \lambda) dt. \tag{3.11}$$

Next, apply the composite right rectangle rule for the integral condition to get

$$u_0 + \sum_{j=1}^N h_j c_j u_j + r = A \tag{3.12}$$

with

$$r = - \sum_{j=1}^N \int_{t_{j-1}}^{t_j} (t - t_{j-1}) \frac{d}{dt} (c(t)u(t)) dt. \tag{3.13}$$

Finally, ignoring  $R_j$  and  $r$  in (3.10) and (3.12), respectively, we get the following discrete scheme

$$\begin{cases} \mathfrak{J}_{\lambda^N}^N U := \varepsilon D^- U_j + f(t_j, U_j, \lambda^N) = 0, & 1 \leq j \leq N, \\ U_0 + \sum_{j=1}^N h_j c_j U_j = A, \\ U_N = B. \end{cases} \quad (3.14)$$

Using the arguments in [80, Lemma 3.1], we can establish the following parameter-uniform stability result for scheme (3.14).

**Lemma 3.3.** *The discrete solution  $\{U, \lambda^N\}$  satisfies the following estimate*

$$\max \{ \|U\|_{\bar{\omega}}, |\lambda^N| \} \leq C (|A| + |B| + \|F\|_{\omega}),$$

where  $F_j = -f(t_j, 0, 0)$ .

Further, similar to the continuous case, we have the following lemma.

**Lemma 3.4.** *For any mesh functions  $(Y, \eta^N)$  and  $(Z, \nu^N)$  such that  $Y_N = Z_N$ ,*

$$(Y_0 - Z_0) + \sum_{j=1}^N h_j c_j (Y_j - Z_j) = \phi,$$

and

$$\mathfrak{J}_{\eta^N}^N Y - \mathfrak{J}_{\nu^N}^N Z = \chi,$$

we have

$$\max \{ \|Y - Z\|_{\bar{\omega}}, |\eta^N - \nu^N| \} \leq C (\|\chi\|_{\omega} + |\phi|).$$

**Proof.** This proof can be readily done using the argument similar to Lemma 3.2 and using Lemma 3.3. □

### 3.3 A priori error analysis

In this section, we derive the general error estimate for scheme (3.14) based on which a number of a priori meshes for problem (3.1) can be constructed that can resolve the layer and produce parameter-uniform numerical approximation for problem (3.1).

The following bound on the derivative of  $u$  proved in [79, Lemma 2.1] is required for the a priori error analysis.

$$|u'(t)| \leq C \left\{ 1 + \frac{1}{\varepsilon} e^{-\frac{\beta t}{\varepsilon}} \right\}, \quad t \in \bar{J}. \quad (3.15)$$

We shall use the following notation for convenience

$$\vartheta(\omega) := \max_{1 \leq j \leq N} \int_{t_{j-1}}^{t_j} \left( 1 + \varepsilon^{-1} e^{-\frac{\beta t}{\varepsilon}} \right) dt. \quad (3.16)$$

**Theorem 3.1.** *Let  $\{u, \lambda\}$  be the solution of (3.1) and  $\{U, \lambda^N\}$  be its approximation using scheme (3.14). Then*

$$\max \left\{ \|U - u\|_{\bar{\omega}}, |\lambda^N - \lambda| \right\} \leq C \vartheta(\omega). \quad (3.17)$$

**Proof.** Using (3.10), (3.12), and (3.14), we get

$$\mathcal{T}_{\lambda^N}^N U - \mathcal{T}_{\lambda}^N u = R_j, \quad \text{and} \quad (U_0 - u_0) + \sum_{j=1}^N h_j c_j (U_j - u_j) = r.$$

Now, for  $t_j \in \omega$ ,

$$|R_j| \leq \frac{1}{h_j} \int_{t_{j-1}}^{t_j} (t - t_{j-1}) |f_t(t, u(t), \lambda) + f_u(t, u(t), \lambda) u'(t)| dt$$

$$\begin{aligned}
 &\leq \frac{C}{h_j} \int_{t_{j-1}}^{t_j} (t - t_{j-1})(1 + |u'(t)|) dt \\
 &\leq C \int_{t_{j-1}}^{t_j} (1 + |u'(t)|) dt \\
 &\leq C \int_{t_{j-1}}^{t_j} (1 + \varepsilon^{-1} e^{-\frac{\beta t}{\varepsilon}}) dt.
 \end{aligned}$$

Also,

$$\begin{aligned}
 |r| &\leq \sum_{j=1}^N \int_{t_{j-1}}^{t_j} c(t) |t - t_{j-1}| |u'(t)| dt \\
 &\leq \|c\|_{\infty} C \sum_{j=1}^N h_j \int_{t_{j-1}}^{t_j} (1 + \varepsilon^{-1} e^{-\frac{\beta t}{\varepsilon}}) dt \\
 &\leq C \vartheta(\omega) \sum_{j=1}^N h_j \\
 &\leq C \vartheta(\omega).
 \end{aligned}$$

Hence, using Lemma 3.4, we have the desired result. □

We can use Theorem 3.1 to construct a number of a priori meshes for problem (3.1).

We here describe standard Shishkin and Bakhvalov meshes.

**Bakhvalov meshes:** There are several ways to construct these meshes. Our construction is based on the equidistribution of the function

$$M_B(s) := \max \left\{ 1, \frac{K}{\varepsilon} e^{-\frac{\beta s}{\varepsilon}} \right\} \quad (3.18)$$

where  $K$  is a positive user chosen constant; that is, the mesh points  $t_j$  are so that

$$\int_0^{t_j} M_B(s) ds = \frac{j}{N} \int_0^1 M_B(s) ds.$$

On this mesh, we have  $\vartheta(\omega) \leq CN^{-1}$ , cf. [10]. Hence, by Theorem 3.1, we get

$$\max \left\{ \|U - u\|_{\bar{\omega}}, |\lambda^N - \lambda| \right\} \leq CN^{-1}.$$

**Shishkin meshes:** Defining the transition point  $\tau_s$  by

$$\tau_s = \min \left\{ \frac{1}{2}, \beta^{-1} \varepsilon \ln N \right\}, \quad (3.19)$$

and placing  $N/2$  subintervals on each  $[0, \tau_s]$  and  $[\tau_s, 1]$ , Shishkin meshes are constructed. The mesh points are defined by

$$t_j = \begin{cases} jh^{(1)}, & j = 0, \dots, N/2, \\ \tau_s + (j - N/2)h^{(2)}, & j = N/2 + 1, \dots, N, \end{cases} \quad (3.20)$$

where  $h^{(1)} = 2\tau_s/N$  and  $h^{(2)} = 2(1 - \tau_s)/N$ .

On this mesh, we have  $\vartheta(\omega) \leq C(N^{-1} \ln N)$ , cf. [10]. Hence, by Theorem 3.1, we get

$$\max \left\{ \|U - u\|_{\bar{\omega}}, |\lambda^N - \lambda| \right\} \leq CN^{-1} \ln N.$$

### 3.4 A posteriori error estimate

In this section, we derive a posteriori error estimate for  $\{U, \lambda^N\}$  which does not require a priori information about the solution of (3.1). Define the piecewise linear interpolant of the numerical solution  $\{U_j\}$  and denote it by  $\tilde{U}$ . Note that  $\tilde{U}$  is continuous on  $\bar{J}$ , linear on each  $[t_{j-1}, t_j]$ , and  $\tilde{U}(t_j) = U_j$ ,  $0 \leq j \leq N$ . Further, we have

$$\tilde{U}(t) = U_j + (t - t_j)D^-U_j.$$

**Theorem 3.2.** Suppose  $\{u, \lambda\}$  is the solution of (3.1),  $\{U, \lambda^N\}$  is the solution of (3.14) on an arbitrary mesh  $\{t_j\}$  and  $\tilde{U}$  is its piecewise linear interpolant. Then

$$\max \left\{ \left\| \tilde{U}(t) - u(t) \right\|_{\infty}, |\lambda^N - \lambda| \right\} \leq C \max_{1 \leq j \leq N} h_j \left\{ 1 + |D^- U_j| + h_j |D^- U_j|^2 \right\}.$$

**Proof.** We define an auxiliary function  $a$  by  $a(t) = f(t, \tilde{U}(t), \lambda^N)$  and suppose  $\tilde{a}$  is its piecewise linear interpolant on  $\bar{\omega}$ , that is,  $a$  is continuous on  $[0, 1]$ , linear on each  $[t_{j-1}, t_j]$  and equal to  $a(t_j)$  at each mesh point  $t_j$ . Further,

$$\tilde{a}(t) = a(t_j) + (t - t_j)D^- a(t_j).$$

Using (3.1) and (3.14), for  $t \in (t_{j-1}, t_j)$ , we have

$$\begin{aligned} \varphi(t) &= \mathcal{T}_{\lambda^N} \tilde{U}(t) - \mathcal{T}_{\lambda} u(t) = \mathcal{T}_{\lambda^N} \tilde{U}(t) = \varepsilon [\tilde{U}(t)]' + f(t, \tilde{U}(t), \lambda^N) \\ &= \varepsilon D^- U_j + \tilde{a}(t) + (a(t) - \tilde{a}(t)) \\ &= \varepsilon D^- U_j + a(t_j) + (t - t_j)D^- a(t_j) + (a(t) - \tilde{a}(t)) \\ &= -(t_j - t)D^- a(t_j) + (a(t) - \tilde{a}(t)). \end{aligned} \quad (3.21)$$

Now we use the arguments in [70, Theorem 4.3] to prove that

$$\|a - \tilde{a}\|_{\infty} \leq C \max_{1 \leq j \leq N} h_j^2 \left\{ 1 + |D^- U_j| + |D^- U_j|^2 \right\} \quad (3.22)$$

and

$$|D^- a(t_j)| \leq C (1 + |D^- U_j|). \quad (3.23)$$

Thus, combining (3.22) and (3.23) with (3.21), we get

$$\|\varphi\|_{\infty} \leq C \max_{1 \leq j \leq N} h_j \left\{ 1 + |D^- U_j| + h_j |D^- U_j|^2 \right\}. \quad (3.24)$$

Next, we consider the integral boundary condition. We proceed as follows

$$\begin{aligned}
 \zeta &= (\tilde{U} - u)(0) + \int_0^1 c(s)(\tilde{U}(s) - u(s))ds \\
 &= \tilde{U}(0) + \sum_{j=1}^N \int_{t_{j-1}}^{t_j} c(s)\tilde{U}(s)ds - A \\
 &= U_0 + \sum_{j=1}^N \int_{t_{j-1}}^{t_j} \left[ c_j + \int_{t_j}^s c'(\rho)d\rho \right] [U_j + (s - t_j)D^-U_j] ds - A \\
 &= \sum_{j=1}^N \int_{t_{j-1}}^{t_j} \left( \int_{t_j}^s c'(\rho)d\rho \right) U_j ds + \sum_{j=1}^N \int_{t_{j-1}}^{t_j} c_j(s - t_j)D^-U_j ds \\
 &\quad + \sum_{j=1}^N \int_{t_{j-1}}^{t_j} \left( \int_{t_j}^s c'(\rho)d\rho \right) (s - t_j)D^-U_j ds.
 \end{aligned} \tag{3.25}$$

Now, we estimate each term separately as follows

$$\begin{aligned}
 \left| \sum_{j=1}^N U_j \int_{t_{j-1}}^{t_j} \left( \int_{t_j}^s c'(\rho)d\rho \right) ds \right| &\leq \sum_{j=1}^N |U_j| |c'(\rho_j)| h_j \int_{t_{j-1}}^{t_j} ds \\
 &\leq \|c'\|_\infty \max_{1 \leq j \leq N} h_j |U_j| \sum_{j=1}^N \int_{t_{j-1}}^{t_j} ds \\
 &\leq C \max_{1 \leq j \leq N} h_j,
 \end{aligned} \tag{3.26}$$

$$\begin{aligned}
 \left| \sum_{j=1}^N \int_{t_{j-1}}^{t_j} c_j(s - t_j)D^-U_j ds \right| &\leq \sum_{j=1}^N |c_j| |D^-U_j| h_j \int_{t_{j-1}}^{t_j} ds \\
 &\leq \|c\|_\infty \max_{1 \leq j \leq N} h_j |D^-U_j| \sum_{j=1}^N \int_{t_{j-1}}^{t_j} ds \\
 &\leq C \max_{1 \leq j \leq N} h_j |D^-U_j|,
 \end{aligned} \tag{3.27}$$

and

$$\left| \sum_{j=1}^N \int_{t_{j-1}}^{t_j} \left( \int_{t_j}^s c'(\eta)d\eta \right) (s - t_j)D^-U_j ds \right| \leq \sum_{j=1}^N |D^-U_j| |c'(\rho_j)| h_j^2 \int_{t_{j-1}}^{t_j} ds$$

$$\begin{aligned}
 &\leq \|c'\|_\infty \max_{1 \leq j \leq N} h_j^2 |D^-U_j| \int_{t_{j-1}}^{t_j} ds \\
 &\leq C \max_{1 \leq j \leq N} h_j^2 |D^-U_j|. \tag{3.28}
 \end{aligned}$$

Using the estimates (3.26)–(3.28) in (3.25), we get

$$|\zeta| \leq C \max_{1 \leq j \leq N} h_j (1 + |D^-U_j|). \tag{3.29}$$

Finally, we apply Lemma 3.2 to get

$$\max \left\{ \left\| \tilde{U}(t) - u(t) \right\|_\infty, |\lambda^N - \lambda| \right\} \leq C \max_{1 \leq j \leq N} h_j \left\{ 1 + |D^-U_j| + h_j |D^-U_j|^2 \right\}.$$

□

### 3.5 The continuous problem (3.3)

The main aim of this section is to present the correct a posteriori error estimation for problem (3.3). We shall require the stability estimate which is given in the following lemma.

**Lemma 3.5.** *For a sufficiently small  $\varepsilon$ , if there exists a positive constant  $c_0$  such that*

$$1 - \mu A^* - \bar{b} B^* \geq c_0 > 0,$$

where

$$A^* = \begin{cases} 0, & \mu \leq 0, \\ \varepsilon e^{-\frac{\beta}{\varepsilon}}, & \mu > 0, \end{cases} \quad B^* = \begin{cases} 0, & \bar{b} \leq 0, \\ \alpha^{-1} \varepsilon (1 - e^{-\frac{\beta}{\varepsilon}}), & \bar{b} > 0, \end{cases}$$

with  $\bar{b} = \max_{t \in \bar{J}} b(t)$ . Then

$$\|u\|_\infty \leq C (\|\mathcal{F}\|_\infty + |d|),$$

where  $\mathcal{F}(t) = -f(t, 0)$ .

**Proof.** See [69, Lemma 2.1]. □

Using arguments similar to the proof of Lemma 3.2, we can prove the following lemma.

**Lemma 3.6.** *For any two functions  $v_1$  and  $v_2$ , and two bounded piecewise continuous functions  $\varphi^*$  and  $\zeta^*$  satisfying*

$$\mathcal{L}v_1 - \mathcal{L}v_2 = \varphi^*,$$

with

$$(v_1 - v_2)(0) = \mu(v_1 - v_2)(1) + \int_0^1 b(s)(v_1 - v_2)(s) ds + \zeta^*,$$

we have

$$\|v_1 - v_2\|_\infty \leq C(\|\varphi^*\|_\infty + |\zeta^*|).$$

**Remark 3.1.** In [70], it is assumed that  $v_1$  and  $v_2$  are two functions such that

$$\begin{aligned} v_1(0) &= \mu v_1(1) + \int_0^1 b(s)v_1(s) ds + d, \\ v_2(0) &= \mu v_2(1) + \int_0^1 b(s)v_2(s) ds + d, \end{aligned}$$

with  $\mathcal{L}v_1 - \mathcal{L}v_2 = \varphi^*$ , where  $\varphi^*$  is a bounded piecewise continuous function. Then,  $\|v_1 - v_2\|_\infty \leq C\|\varphi^*\|_\infty$ . This estimate is utilized in their a posteriori error analysis, where  $v_1$  is replaced with the piecewise linear interpolant  $\tilde{U}$  of the discrete solution  $U$  and  $v_2$  is replaced with the exact solution  $u$ . Note that  $\tilde{U}$  cannot satisfy the integral boundary condition exactly. Hence, it is wrongly assumed in [70].

On an arbitrary nonuniform mesh  $\bar{\omega} \equiv \{0 = t_0 < \dots < t_N = 1\}$  the following discretization of (3.3) is considered in [70]:

$$\begin{cases} \varepsilon D^-U_j + f(t_j, U_j) = 0, & 1 \leq j \leq N, \\ U_0 = \mu U_N + \sum_{j=1}^N h_j b_j U_j + d. \end{cases} \quad (3.30)$$

The following lemma shows that the above discretization is parameter-uniform stable.

**Lemma 3.7.** *For a sufficiently small  $\varepsilon$ , if there exists a positive constant  $\bar{c}_0$  such that  $1 - \mu P_N - \sum_{j=1}^N h_j b_j P_j \geq \bar{c}_0 > 0$ , where  $P_j = \prod_{k=1}^j \frac{\varepsilon}{\varepsilon + a_k h_k}$  with  $a_k = \frac{\partial f}{\partial u}(t_k, U_k + \gamma U_k)$ ,  $0 < \gamma < 1$ . Then*

$$\|U\|_{\bar{\omega}} \leq C (\|\mathcal{F}\|_{\omega} + |d|), \quad (3.31)$$

where  $\mathcal{F}_j = -f(t_j, 0)$ .

**Proof.** We can obtain this result by proceeding similarly as in [70, Lemma 4.3].  $\square$

**Theorem 3.3.** *Suppose  $u$  is the solution of (3.3),  $U$  is the solution of (3.30) on an arbitrary mesh  $\{t_j\}$  and  $\tilde{U}$  is its piecewise linear interpolant. Then*

$$\|\tilde{U} - u\|_{\infty} \leq C \max_{1 \leq j \leq N} h_j \left\{ 1 + |D^-U_j| + h_j |D^-U_j|^2 \right\}.$$

**Proof.** Note that  $\tilde{U}$  is continuous on  $\bar{J}$ , linear on each  $[t_{j-1}, t_j]$  and  $\tilde{U}(t) = U_j + (t - t_j)D^-U_j$ . It is shown in [70, Theorem 4.3] that for  $\varphi^*(t) = \mathcal{L}\tilde{U}(t) - \mathcal{L}u(t)$ ,

$$\|\varphi^*\|_{\infty} \leq C \max_{1 \leq j \leq N} \left\{ h_j \left( 1 + |D^-U_j| + h_j |D^-U_j|^2 \right) \right\}. \quad (3.32)$$

However, what follows is missing in [70, Theorem 4.3]. We proceed as follows for the integral boundary condition

$$\begin{aligned}
 \zeta^* &= (\tilde{U} - u)(0) - \mu(\tilde{U} - u)(1) - \int_0^1 b(s)(\tilde{U}(s) - u(s))ds \\
 &= \tilde{U}(0) - \mu\tilde{U}(T) - \int_0^T b(s)\tilde{U}(s)ds - d \\
 &= U_0 - \mu U_N - \sum_{j=1}^N \int_{t_{j-1}}^{t_j} b(s)\tilde{U}(s)ds - d \\
 &= U_0 - \mu U_N - \sum_{j=1}^N \int_{t_{j-1}}^{t_j} \left[ b_j + \int_{t_j}^s b'(\eta)d\eta \right] [U_j + (s - t_j)D^-U_j] ds - d \\
 &= - \sum_{j=1}^N \int_{t_{j-1}}^{t_j} \left( \int_{t_j}^s b'(\eta)d\eta \right) U_j ds - \sum_{j=1}^N \int_{t_{j-1}}^{t_j} b_j(s - t_j)D^-U_j ds \\
 &\quad - \sum_{j=1}^N \int_{t_{j-1}}^{t_j} \left( \int_{t_j}^s b'(\eta)d\eta \right) (s - t_j)D^-U_j ds. \tag{3.33}
 \end{aligned}$$

All the above terms are estimated as follows

$$\begin{aligned}
 \left| \sum_{j=1}^N U_j \int_{t_{j-1}}^{t_j} \left( \int_{t_j}^s b'(\eta)d\eta \right) ds \right| &\leq \sum_{j=1}^N |U_j| \|b'(\eta_j)\| h_j \int_{t_{j-1}}^{t_j} ds \\
 &\leq \|b'\|_\infty \max_{1 \leq j \leq N} h_j |U_j| \sum_{j=1}^N \int_{t_{j-1}}^{t_j} ds \\
 &\leq C \max_{1 \leq j \leq N} h_j, \tag{3.34}
 \end{aligned}$$

$$\begin{aligned}
 \left| \sum_{j=1}^N \int_{t_{j-1}}^{t_j} b_j(s - t_j)D^-U_j ds \right| &\leq \sum_{j=1}^N |b_j| |D^-U_j| h_j \int_{t_{j-1}}^{t_j} ds \\
 &\leq \|b\|_\infty \max_{1 \leq j \leq N} h_j |D^-U_j| \sum_{j=1}^N \int_{t_{j-1}}^{t_j} ds \\
 &\leq C \max_{1 \leq j \leq N} h_j |D^-U_j|, \tag{3.35}
 \end{aligned}$$

and

$$\begin{aligned}
 \left| \sum_{j=1}^N \int_{t_{j-1}}^{t_j} \left( \int_{t_j}^s b'(\eta) d\eta \right) (s - t_j) D^- U_j ds \right| &\leq \sum_{j=1}^N |D^- U_j| |b'(\eta_j)| h_j^2 \int_{t_{j-1}}^{t_j} ds \\
 &\leq \|b'\|_\infty \max_{1 \leq j \leq N} h_j^2 |D^- U_j| \sum_{j=1}^N \int_{t_{j-1}}^{t_j} ds \\
 &\leq C \max_{1 \leq j \leq N} h_j^2 |D^- U_j|. \tag{3.36}
 \end{aligned}$$

On combining the estimates (3.34)–(3.36) together with (3.33), we get

$$|\zeta^*| \leq C \max_{1 \leq j \leq N} h_j (1 + |D^- U_j|). \tag{3.37}$$

Now apply Lemma 3.6 and obtain

$$\|\tilde{U} - u\|_\infty \leq C \max_{1 \leq j \leq N} h_j \left\{ 1 + |D^- U_j| + h_j |D^- U_j|^2 \right\}. \tag{3.38}$$

□

## 3.6 Numerical results

This section is dedicated to numerical experimentation of the methods proposed in this chapter. The following two test examples are considered.

**Example 3.1.** *Consider the test problem*

$$\begin{cases} \varepsilon u'(t) + 2u - e^{-u} + t^2 + \lambda + \tanh(\lambda + t) = 0, & t \in (0, 1], \\ u(0) + \frac{1}{4} \int_0^1 e^{-s} u(s) ds = 1, \\ u(1) = 0. \end{cases}$$

**Example 3.2.** *Consider the test problem*

$$\begin{cases} \varepsilon u'(t) + u - e^{-u} - \lambda - t = 0, & t \in (0, 1], \\ u(0) + \int_0^1 e^{-2s} u(s) ds = 1, \\ u(1) = 0. \end{cases}$$

We use the following iterative scheme to solve the nonlinear system of algebraic equation corresponding to (3.12). This iterative scheme is similar to Newton's method (see [127–129]) and has been used previously in [69, 80]:

$$\begin{cases} \lambda^{(k)} = \frac{\frac{\varepsilon}{h_j}(U_{N-1}^{(k)} - B) + \frac{\partial f}{\partial \lambda}(1, B, \lambda^{(k-1)})\lambda^{(k-1)} - f(1, B, \lambda^{(k-1)})}{\frac{\partial f}{\partial \lambda}(1, B, \lambda^{(k-1)})}, \\ U_0^{(k)} = A - h_N c_N B - \sum_{j=1}^{N-1} h_j c_j U_j^{(k-1)}, \\ U_j^{(k)} = \frac{\frac{\varepsilon}{h_j} U_{j-1}^{(k)} + \frac{\partial f}{\partial u}(t_j, U_j^{(k-1)}, \lambda^{(k)}) U_j^{(k-1)} - f(t_j, U_j^{(k-1)}, \lambda^{(k)})}{\frac{\varepsilon}{h_j} + \frac{\partial f}{\partial u}(x_j, U_j^{(k-1)}, \lambda^{(k)})}, \end{cases}$$

$j = 1, \dots, N - 1, k = 1, 2, \dots$ ;  $U_j^{(0)}$  and  $\lambda^{(0)}$  are initial iterations. The stopping criterion is taken to be

$$\max \left\{ \max_j \left| U_j^{(k)} - U_j^{(k-1)} \right|, \left| \lambda^{(k)} - \lambda^{(k-1)} \right| \right\} \leq 10^{-8}$$

and the initial guess in the iteration process is taken as  $U_j^{(0)} = 1 - t_j^2$ ,  $\lambda^{(0)} = -0.4$  for both the test examples.

The a posteriori error estimates derived in the present chapter can underlie any reliable a posteriori mesh construction algorithm. Here we consider adaptive mesh construction algorithm originally proposed by De Boor [40]. Starting with a uniform

mesh the algorithm constructs a mesh that solves the equidistribution problem

$$h_j \psi_j = \frac{1}{N} \sum_{i=1}^N h_i \psi_i, \quad j = 1, \dots, N. \quad (3.39)$$

where the monitor function  $\psi$  is chosen from the a posteriori error estimate. For the present problem,  $\psi_j = 1 + |D^-U_j| + h_j |D^-U_j|^2$ , as suggested by Theorem 3.2. It was pointed out in [43] that it is not necessary to enforce (3.39) strictly. It is sufficient to stop the algorithm when the following weakened equidistribution principle

$$h_j \psi_j \leq \frac{C_0}{N} \sum_{i=1}^N h_i \psi_i, \quad j = 1, \dots, N, \quad (3.40)$$

where  $C_0 > 1$  is some user chosen constant. To solve the weakened equidistribution problem (3.40), we use the Algorithm 2 originally due to De Boor [40]. In literature, it has been utilized for several classes of singularly perturbed problems (see [43, 46] and the references therein). The convergence of the algorithm is studied in [43, 130] for singularly perturbed problems and in [131] for regular boundary value problems.

We use the set  $E_\varepsilon = \{\varepsilon \mid \varepsilon = 2^{-2}, 2^{-6}, \dots, 2^{-30}\}$ . For both the test examples, we do not have the exact solution. Therefore, to estimate the errors and convergence rates we use the double mesh principle. For different values of  $\varepsilon$  and  $N$ , we compute the numerical solution  $\{U^{\varepsilon,N}, \lambda^{\varepsilon,N}\}$  and then bisect the mesh used for it to compute another numerical solution  $\{U^{\varepsilon,2N}, \lambda^{\varepsilon,2N}\}$ . Then the maximum pointwise errors are calculated by using the formula

$$G^{\varepsilon,N} = \max\{G_u^{\varepsilon,N}, G_\lambda^{\varepsilon,N}\},$$

where

**Algorithm 2:** A posteriori mesh construction

**Input:**  $N \in \mathbb{N}$ ,  $0 < \varepsilon \leq 1$ ,  $C_0 = 1.01$ , and the discrete monitor function  $\psi_j$ .

**Output:** Equidistribution mesh  $\{t_j\}$  and the solution  $\{U_j, \lambda^N\}$ .

Step 1. Define  $t_j^{(0)} = j/N$ ,  $j = 0, \dots, N$ , as the initial iteration of the adaptive mesh ( $r = 0$ ).

Step 2. Solve the discrete problem (3.12) on  $\{t_j^{(r)}\}$  to get the solution  $\{U_j^{(r)}, \lambda^{N,(r)}\}$ .

Step 3. Set  $h_j^{(r)} = t_j^{(r)} - t_{j-1}^{(r)}$  and evaluate the monitor function

$$\psi_j^{(r)} = 1 + |D^-U_j^{(r)}| + h_j^{(r)}|D^-U_j^{(r)}|^2, \quad \text{for } j = 1, \dots, N.$$

$$\text{Compute } \Psi_j^{(r)} = \sum_{i=1}^j h_i^{(r)} \psi_i^{(r)}.$$

Step 4. Stopping criteria: go to Step 6, if  $\max_{1 \leq j \leq N} h_j^{(r)} \psi_j^{(r)} \leq C_0 \frac{\Psi_N^{(r)}}{N}$ ; else continue with the next step.

Step 5. Set  $\xi_j^{(r)} = j \frac{\Psi_N^{(r)}}{N}$  for  $j = 0, \dots, N$ . Generate a new mesh  $\{t_j^{(r+1)}\}$  by interpolating the points  $(\Psi_j^{(r)}, t_j^{(r)})$  and evaluating this interpolant at  $\xi_j^{(r)}$  for  $j = 0, 1, \dots, N$ . Return to Step 2 setting  $r = r + 1$ .

Step 6. Take  $\{t_j^{(r)}\}$  as the final adaptive mesh and  $\{U_j^{(r)}, \lambda^{N,(r)}\}$  as the adaptive solution. Stop.

Mesh	$\varepsilon \in E_\varepsilon$	$N = 32$	$N = 64$	$N = 128$	$N = 256$	$N = 512$	$N = 1024$
Shishkin mesh	$G^N$	9.2829e-03	5.9200e-03	3.6160e-03	2.1330e-03	1.2211e-03	6.8465e-04
	$\varrho^N$	0.6490	0.7112	0.7615	0.8047	0.8347	
Bakhvalov mesh	$G^N$	4.5213e-03	2.3324e-03	1.1856e-03	5.9794e-04	3.0025e-04	1.5045e-04
	$\varrho^N$	0.9549	0.9762	0.9875	0.9938	0.9969	
A posteriori mesh	$G^N$	9.8906e-03	5.5733e-03	3.0810e-03	1.6411e-03	8.5560e-04	4.4046e-04
	$\varrho^N$	0.8209	0.8498	0.9087	0.9397	0.9579	

TABLE 3.1: Parameter-uniform errors and rates of convergence for Example 3.1.

$$G_u^{\varepsilon,N} = \max_{0 \leq j \leq N} |U_j^{\varepsilon,N} - U_{2j}^{\varepsilon,2N}|, \quad G_\lambda^{\varepsilon,N} = |\lambda^{\varepsilon,N} - \lambda^{\varepsilon,2N}|,$$

and parameter-uniform errors and rates of convergence are calculated by

$$G^N = \max_{\varepsilon} \{G^{\varepsilon, N}\}, \quad \text{and} \quad \varrho^N = \log_2 (G^N / G^{2N}),$$

respectively.

Tables 3.1 and 3.2 display parameter-uniform errors and rates of convergence on both a priori (Shishkin and Bakhvalov) and a posteriori meshes for Examples 3.1 and 3.2, respectively. From these tables, one can observe that the errors are larger on Shishkin mesh than on Bakhvalov and a posteriori mesh, which is not surprising as the error bound on Shishkin mesh has an extra logarithmic factor in comparison to the error bounds of Bakhvalov mesh and a posteriori mesh. Further, these tables confirm the

Mesh	$\varepsilon \in E_{\varepsilon}$	$N = 32$	$N = 64$	$N = 128$	$N = 256$	$N = 512$	$N = 1024$
<b>Shishkin mesh</b>	$G^N$	4.8965e-02	3.3310e-02	2.1149e-02	1.2791e-02	7.4554e-03	4.2359e-03
	$\varrho^N$	0.5558	0.6554	0.7254	0.7788	0.81561	
<b>Bakhvalov mesh</b>	$G^N$	3.5295e-02	2.2093e-02	1.3030e-02	7.2020e-03	3.8338e-03	2.0002e-03
	$\varrho^N$	0.6759	0.7618	0.8554	0.9096	0.9386	
<b>A posteriori mesh</b>	$G^N$	3.0635e-02	1.6249e-02	8.7552e-03	4.5368e-03	2.3226e-03	1.1822e-03
	$\varrho^N$	0.9148	0.8922	0.9485	0.9659	0.9742	

TABLE 3.2: Parameter-uniform errors and rates of convergence for Example 3.2.

first order accuracy of (3.14) on Bakhvalov mesh and on a posteriori constructed mesh. Note that the construction of Bakhvalov mesh requires sufficient knowledge about the location and width of the boundary layer, while the construction of a posteriori mesh does not require this information.

In addition, we provide the log-log plot of the maximum pointwise errors for both the test examples in Figure 3.1. Slopes of these plots matches with the slopes of the theoretical order plots, which again authenticates our theoretical findings.

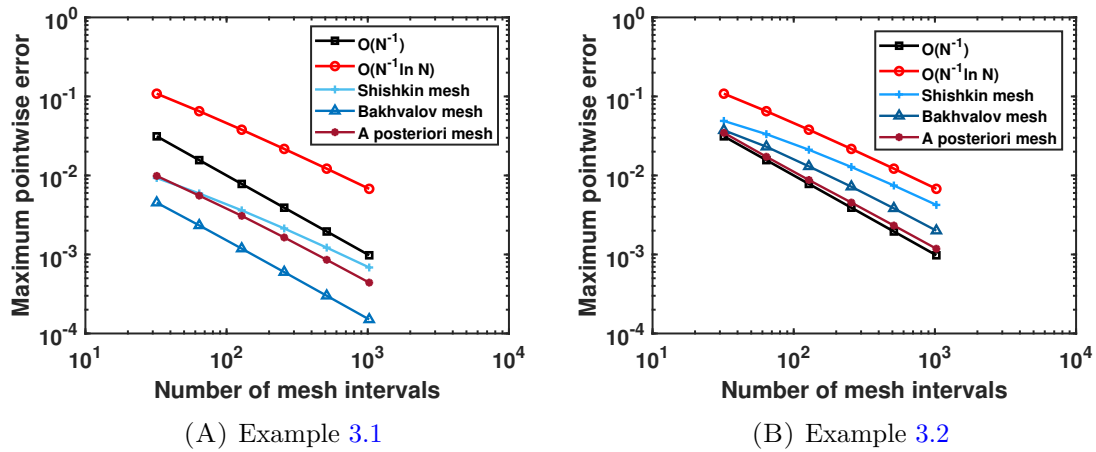


FIGURE 3.1: Log-log plots of errors vs  $N$  for  $\varepsilon = 2^{-20}$ .

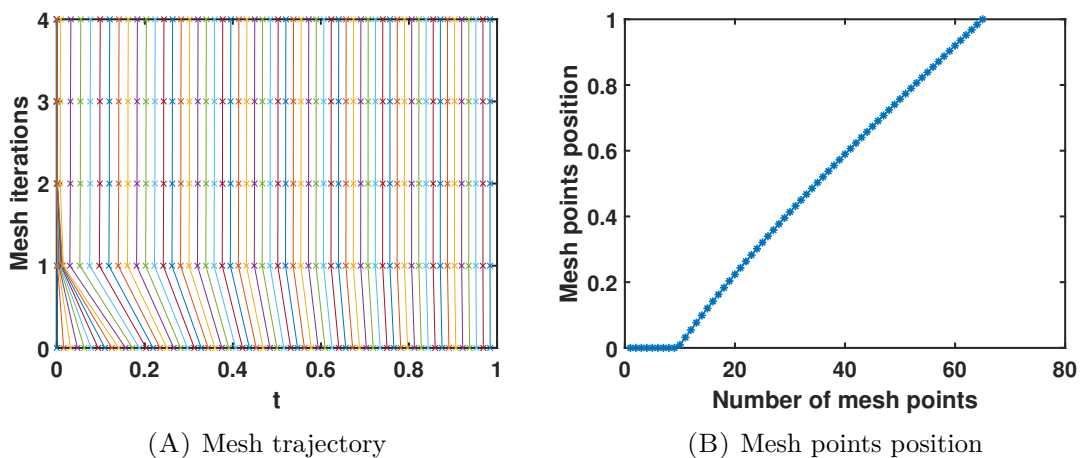


FIGURE 3.2: Movement of mesh points along mesh iterations and the final adaptive mesh position taking  $N = 64$  and  $\varepsilon = 2^{-20}$  for Example 3.1.

Next, to show the adaptive nature of the a posteriori constructed mesh, in Figure 3.2, we have given the trajectory of the mesh points and the position of the final mesh points. Here, we can clearly see that the mesh points are condensing towards the left side and finally adapts the solution behavior by itself. This confirms the adaptivity of a posteriori constructed mesh.

## 3.7 Conclusions

A nonlinear singularly perturbed parameterized problems with integral boundary condition is considered. The discretization comprises of an implicit Euler scheme for the nonlinear problem, and a composite right rectangle rule for the integral boundary condition. We conducted the a priori as well as a posteriori error analysis for the proposed discrete scheme. Numerical experiments are performed and results are reported for validation of the theoretical error estimates.

